16th ICAAR LISBOA 2020-2022

16th International Conference on
Alkali-Aggregate Reaction in Concrete
Lisboa | LNEC | Portugal | 31 May - 2 June 2022

http://icaar2020-2022.lnec.pt

Profiling the internal damage within an ASR-affected dam component with the Damage Rating Index (DRI)

Mathieu Champagne [(1)], Jan Lindgård [(2)], Benoit Fournier [(3)], Benoit Bissonnette [(4)], Carl Duchesne [(5)]

(1) *Laval University, Québec City, Canada, mathieu.champagne.8@ulaval.ca*

(2) SINTEF Building and Infrastructure, Trondheim, Norway, jan.lindgard@sintef.no

(3) *Laval University, Québec City, Canada, benoit.fournier@ggl.ulaval.ca*

(4) *Laval University, Québec City, Canada, carl.duchesne@gch.ulaval.ca*

(5) *Laval University, Québec City, Canada, benoit.bissonnette@gci.ulaval.ca*

Abstract

A proper assessment of the extent of reaction and damage is essential to select and implement appropriate management actions on structures affected by alkali-silica reaction. Damage assessment of ASR-affected structures is often conducted from the testing of cores extracted in the outer portion (i.e. at limited depth) within structural elements showing visual symptoms associated to this pathology However, there is no certainty that the condition of the core section examined/tested actually provides a real indication of the condition of the whole structural element investigated. This paper presents an approach to apply the Damage Rating Index (DRI) for spatial analysis and the establishment of an internal damage profile in ASR-affected concrete structures/components. The above profile is obtained by segmenting the extracted core in *DRI zones* of similar area along the examined core, assessing their respective DRI number and referencing the obtained values with their distance from the surface of the component. This damage spatial analysis tool was applied to a ±2.3 m long core extracted from the bottom portion of the abutment wall of a Norwegian ASR-affected dam.

The main finding of this study is that internal damage varied significantly at the scale of one hundred mm within the assessed component. Although damage variations were noticed at a relatively small scale, six different damage zones were noticed inside the component, which are assumed to be caused by the influence of the freeze/thaw in conjunction with ASR at the downstream surface and the anisotropic restraints inside the dam (and the resulting heterogeneous tensile/compressive stresses).

***Keywords**: ASR, damage rating index; internal damage; diagnosis.*

1. INTRODUCTION

The condition of concrete structures affected by alkali-silica reaction (ASR) needs to be assessed from durability and, in severe cases, from structural point of views. This can be very challenging for engineers because the rate and extent of expansion/cracking can vary significantly from an affected structure to another and even between structural elements of a single structure [1]. From an owner's perspective, the reliable assessment of the extent of reaction and damage is essential to select/implement appropriate management actions while minimizing their socio-economic and safety impacts [2, 3]. This stage in the management of an ASR-affected structure is referred as *Diagnosis*. Common practice generally consists in extracting cores from the "surficial zone" of a structural component showing visual symptoms of deterioration generally associated with the pathology suspected, thus assuming that it is somewhat representative of its internal condition. However, this assumption is rarely verified and can possibly lead to incorrect management actions. In this paper, the Damage Rating Index (DRI), a commonly used damage assessment tool for ASR affected structures in North America [4], was applied to profile the internal damage and reliably (i.e. with enough sensitivity) assess how it varies/progresses within a relatively thick element of an ASR-affected dam.

1.1 Damage Rating Index (DRI)

The DRI method was developed in the 1990's by P.E. Grattan-Bellew from the National Research Council of Canada [5]. It is a semi-quantitative petrographic (i.e. visual) tool performed with the use of a stereomicroscope (about 15× magnification) where damage features generally associated with ASR are counted by an operator through a 1-2 cm² grid drawn on the surface of a polished section. The number of counts corresponding to each selected petrographic feature is multiplied by weighting factors, whose purpose is to balance their relative importance with respect to the distress mechanism of interest, for instance ASR [3]. Each square is thereby summed up to obtain a numerical value, the *DRI number*, which is normalized to a 100 cm² area for ease of comparison.

The weighting factors proposed in the original method [5] were chosen arbitrarily, but on a logical basis for ASR-related damage assessment [3, 6]. Since then, the method was performed in many research programs but was slightly changed in various ways. This is a consequence of the absence of a standard practice for this method up to this day. For instance, some used a grid size of 15 mm [7–9], while others selected 10 mm [3, 6, 10]. Also, some researchers stained the polished section to help identifying the cracks [9, 11], as originally proposed by Grattan-Bellew and Danay [5]. Moreover, different weighting factors were used and some even included new features, such as *corroded particles* [6] or *cracks extending into the cement paste* [12]. Consequently, it is difficult to compare results of studies carried out in different labs. For example, Grattan-Bellew [10] mentioned that a DRI number greater than 50 is considered to indicate significant deterioration of concrete, whereas Sanchez et al. [13] consider this severity level of deterioration at a DRI number of approximately 500.

Although many other weighting factors were used in the past, probably the most cited studies for the basis of selecting weighting factors are the so-called "traditional" and "modified" methods of Grattan-Bellew and Mitchell [11] and Villeneuve et al. [6], respectively (Table 1.1). The "traditional" method offers a diagnosis-oriented approach with a distinction in the weighing factors associated to cracks with or without reaction products as well as including reaction rims around particles and reaction products in voids of the cement paste in the counted symptoms. On the other hand, the "modified" method focuses more on damage/cracking assessment and its weighting factors were selected with the purpose of decreasing the inter-operator variability. The vast majority of recent studies involving DRI (e.g. [3, 14–16]) applied the "modified" method (i.e. set of weighing factors, sample preparation and grid size), thus allowing to compare the results of damage assessment studies carried out by different groups and setting the base for standardization of the method. Two damage classifications for ASR were proposed for the "modified" DRI method by Sanchez et al. [13] and Fournier et al. [17] (Table 1.2). The former has five levels and is based on the correlation between the DRI number and other parameters such as expansion and mechanical properties losses measured on a wide range of laboratory specimens manufactured with different compressive strengths and reactive aggregates. The latter was based on the petrographic examination of about 75 concrete cores extracted from the piers of a concrete bridge affected by ASR in Eastern Canada. The four levels of ASR severity were based on the general changes of ASR stage observed in the concrete.

Table 1.1: Petrographic features along with some weighing factors used in the determination of the DRI number.

Petrographic features		Acronyms	Weighing factor	
			[11]	[6]
Crack in the aggregate particles (> 1 mm)	*Closed (without reaction products)*	**CCA**	**0.75**	**0.25**
	Opened or in a fine network (without reaction products)	**OCA**	**4**	**2**
	Opened or in a fine network (with reaction products)	**CA + RP**	**2**	**2**
Crack in the cement paste	*Without reaction products*	**CCP**	**2**	**3**
	With reaction products	**CCP + RP**	**4**	**3**
Debonded aggregate particle (> 1 mm)		**Debon**	**3**	**3**
Reacted aggregate particle (> 1 mm)		**RAP**	**---**	**2**
Reaction rim (> 1 mm)		**RR**	**0.5**	**---**
Reaction products in voids of the cement paste		**RPV**	**0.5**	**---**

A recent study carried out at Laval University introduced an approach to apply the DRI method for the reliable assessment of "damage zonings" in field specimens extracted from concrete structure components [18]. However, this new damage assessment tool, which is further detailed in section 4.2,

had yet to be applied to case studies where sufficiently long cores are available for this type of analysis with the DRI method.

Table 1.2: ASR damage classification for the DRI using weighing factors proposed by Villeneuve et al. [6], adapted from Sanchez et al. [13] (laboratory) and Fournier et al. [17] (field structure).

Adapted from Sanchez et al. [13] – based on laboratory investigations					Fournier et al. [17] – field structure	
Damage classification for ASR	Reference expansion (%)	Stiffness loss (%)	Compressive strength loss (%)	DRI	DRI	Damage classification for ASR
Negligeable	0.00-0.03	--	--	< 155	< 200/250	Trace
Marginal	0.04 ± 0.01	5-37	(-) 10-15	210-400	200/250-400	Fair to moderate
Moderate	0.11 ± 0.01	20-50	0-20	330-500		
High	0.20 ± 0.01	35-60	13-25	500-765	400-700/750	Moderate to severe
Very high	0.30 ± 0.01	40-67	20-35	600-925	>700-750	Severe to very severe

2. SCOPE OF WORK AND OBJECTIVES

During the summer of 2015, an extensive repair work was performed on the Votna I dam, an ASR-affected dam in the south-western part of Norway (at an altitude of about 1000 m above sea level), to release the high compressive stresses at the connection point between the arch dam, the abutment wall and the slab dam (Figure 2.1). The reservoir was emptied during that period, thus allowing to extract large concrete sections and cores at different locations that would not be accessible otherwise, i.e. always or from time to time underwater (depending on the level of the reservoir). During the repair period, an extensive research project was carried out to assess the internal damage, alkali content and moisture state at different locations within the structure [19]. This paper presents the results of the detailed damage assessment performed along a ≈2.3 meter-long core that was recovered from the bottom part of the structure with the objective of assessing how the internal damage varies at different depths (from the surface to the interior of the dam) within the ASR-affected dam.

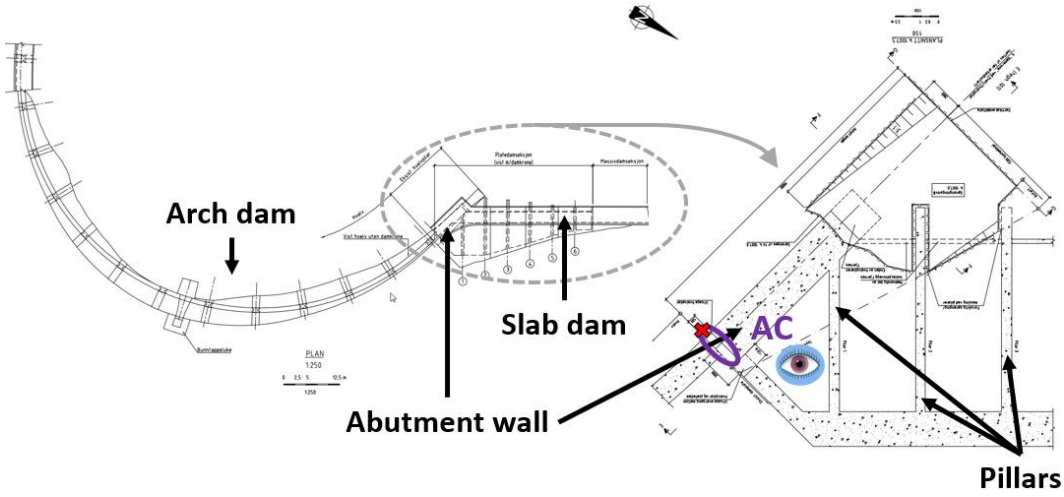

Figure 2.1: Sketch of the Votna I Dam (top view) and location of the extracted core (called “AC”). The red cross indicates the reference surface of the core. The arrow at the top points the north direction. The eye is the position of the view inside the dam in Figure 3.1A (adapted from Plusquellec et al. [19]).

3. MATERIALS

3.1 Votna I dam

Votna I dam was built between 1964 and 1966. It is a double-curved arch dam connected to a slab dam via an abutment wall, as shown in Figure 2.1 [19]. The water level in the reservoir reaches the top of the dam during summer/fall and decreases gradually during winter/spring. The approximate concrete mix-design used for the slab dam consisted of 350 kg/m^3 of ordinary portland cement (OPC), 930 kg/m^3 of sand (0/-8 mm), 950 kg/m^3 of coarse aggregate (8/-50 mm) and 190 kg/m^3 of free water [19], but the composition may slightly differ from one location to another. The coarse aggregate used is classified as potentially reactive according to the Norwegian regulations; it consists of a cataclastic crushed rock locally excavated from the (now) submerged area upstream of the Votna I dam.

The first indications of ASR in the dam, consisting of typical map cracking and deformation, were noticed in the years 1987-1988 and later confirmed by Rodum et al. [20] and Larsen et al. [21]. SINTEF and the consultant company Sweco performed an extensive laboratory investigation on Votna I including damage assessment, moisture state, mechanical properties and safety evaluations [21]. They concluded that the reaction was still in an early state and a satisfactory capacity of the arch will be maintained for at least 20 years (from 2008).

The repair works undertaken during the summer of 2015 consisted of cutting out parts from the slab dam (≈1-meter width) and the abutment wall (≈0.5-meter width) perpendicularly to one another and over their entire height (≈15-16 meters) to release stresses at their junction. This was done in June 2015 by sequentially cutting and removing blocks of approximately 2 m^3 from the above locations. Figure 3.1A shows a view from inside of the dam (location marked by an eye in Figure 2.1) after the blocks were removed from the slab dam.

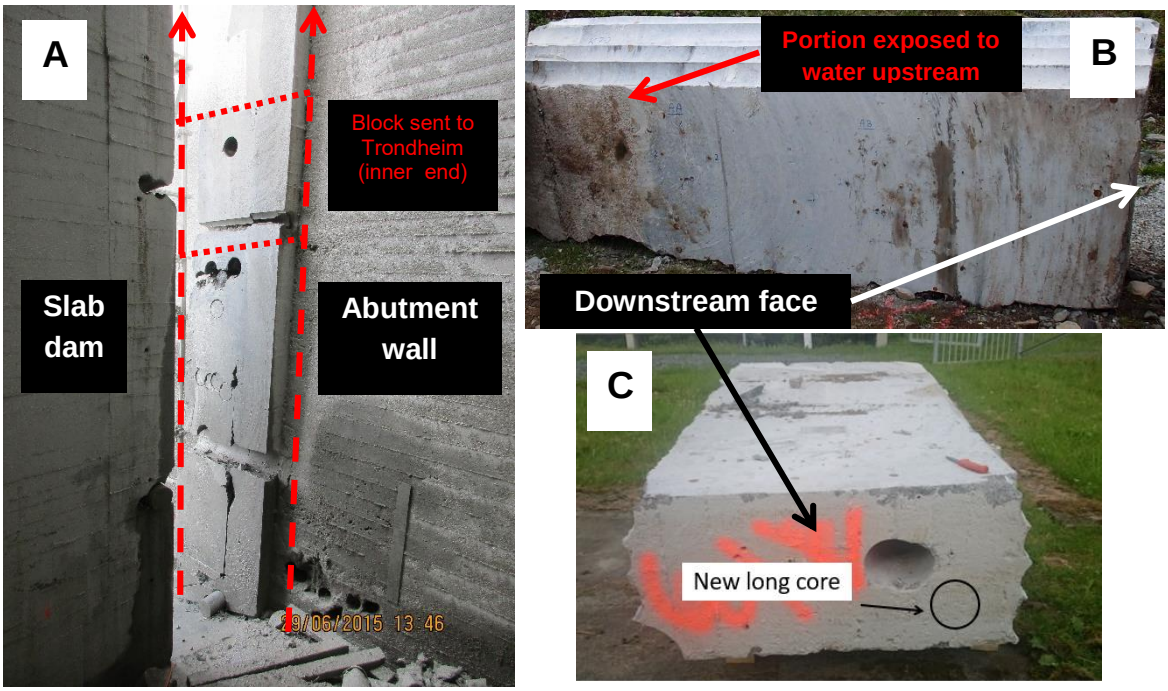

Figure 3.1: (A) View from inside of the dam after the blocks were removed from the slab dam and before the blocks were removed from the abutment wall (The red arrows indicate the direction of cutting). (B) View of an abutment wall block removed from the dam showing the 500 mm long portion exposed to water on the left. (C) Location of the extracted core from the abutment wall block stored at SINTEF's field exposure site at Voll in Trondheim (Norway).

3.2 The core specimen

One relatively large block extracted from the lower part of the abutment wall was sent to SINTEF's field exposure site at Voll in Trondheim (Norway). The block was located very close to the connection point

where the slab dam meets the abutment wall and the arch dam, as shown in Figure 2.1 (marked as "AC"). The block was exposed to atmospheric conditions on the downstream face while the last 500 mm on the other side of the block, i.e. towards the upstream face, was directly exposed to water on one of its faces (Figure 3.1B). In November 2015, a 150 mm-diameter core was extracted over the entire length of the block (≈2.3 m) to assess its internal damage. Considering the coring location in the block (Figure 3.1C), the “concrete cover’ from the water (reservoir) was only about 100 mm for the last 500 mm of the core (Figure 3.1B). The extracted core is shown in Figure 3.2 (broken into six pieces). The core sections were cut lengthways and polished using a portable wet stone grinder with a range of diamond-impregnated wet resin polishing pads (no free grit material). The polished sections (specimens) were then photographed, and a grid was drawn on the sections, with squares of 10 mm by 10 mm in size, as recommended by Villeneuve et al. [6].

Figure 3.2: Extracted core (broken in six pieces) from the block shown in Figure 3.1C; the reference surface (to the left) is the downstream face (red cross in Figure 2.1) and the white arrows indicate the presence of reinforcing bars.

4. METHODS

4.1 Damage Assessment

The DRI method was applied along the ≈2.3 meter-long core. The whole area of the polished specimens was examined under the stereomicroscope at ±15× magnification, except the most external lines along the longitudinal axis of the core to avoid detrimental effects from coring or polishing operations [18]. The petrographic features and their related weighing factors proposed by Villeneuve et al. [6] were applied for the determination of the DRI numbers (Table 1.1). The DRI numbers obtained with these weighing factors were found to reliably assess damage of concrete due to ASR in terms of expansion [3] and loss in mechanical properties [14]. The cracks were counted in the coarse aggregate and sand particles larger than 1 mm in diameter to consider also the reactivity of the sand (if any), as recommended by Sanchez et al. [22].

4.2 Internal damage profiling approach

The internal damage profile approach introduced by Champagne [18] is illustrated in Figure 4.1. The downstream face was chosen as the spatial reference point. Then, a step-by-step approach was used for establishing a damage profile through the analysis of *DRI zones* located at increasing distances from that reference point. The DRI number obtained for each zone was assigned to its middle point in reference to its distance from the extraction surface. The size of the zones and hence the number of DRI values obtained over the whole core was dictated by a “step distance”, i.e. the number of squares selected along the longitudinal axis of the core. Based on the author’s experience and some preliminary testing, a step distance of 60 mm was applied in this study. As illustrated on Figure 4.1, the first DRI value was obtained for the area corresponding to “one” step distance from the extraction surface. Then, the subsequent DRI values were systematically calculated from zones corresponding to the preceding step distance plus “one” step distance forward (Figure 4.1). The above process was then continued until reaching the end of the core. The first (smaller) zone was chosen for properly assessing the local damage difference that is expected near the surface compared to the interior of the concrete element [18].

4.3 Statistical approach to address theoretical variability between extracted cores

Champagne [18] also investigated how DRI data collected at the scale of each square can be statistically analysed to address the precision level of the DRI values obtained (by the same operator) through the internal damage profiling approach (section 4.2). The author conducted conventional statistical

treatment on test units composed of 10 to 16 squares (depending on the applied step distance) in each DRI zones and determined the correction factor given in Table 4.1 for the standard deviation thus obtained. The above correction factor (90% confidence level) is proposed to more accurately (statistically) represent the "true" damage level within a concrete member based on the examination of one single core when considering the inherent variability in damage that can be observed at similar depth within that member. It was determined from the analysis of four to six cores extracted close to one another (i.e. within an area/volume where the damage is not expected to vary significantly due to any "external/internal" effects) of seven ASR-affected elements in the field [18].

The optimal way to select "test units" varies from one extraction location to another, although it tends to depend on the depth of the investigated DRI zone [18]. For DRI zones with a high damage gradient, group of consecutive squares parallel to the extraction surface, referred as *lines*, was found to be more precise than a random selection of an equal number of squares [23].

Table 4.1: Suggested standard deviation correction for different step distances and different depths of the center of the assessed DRI zone [18].

Step distance (mm)	50			**60**			70			80		
Depth of the zone center (mm)	25-100	150-400	>400	**30**	**60-360**	**>360**	35	35-350	>350	40	80-320	>320
Standard deviation correction factor	1.60	1.97	1.96	**1.61**	**1.84**	**2.08**	1.71	1.82	2.02	1.57	1.81	2.21

To reliably detect damage variations along the length of the assessed core, a Student confidence interval (90% confidence level) of the "true" value was calculated for each zone of the internal damage profile by determining the standard deviation between test units of 12 squares assessed in the investigated DRI zones. Based on sampling analysis previously performed on this specimen (see Vot. V-7/3 specimen in [18]), sampling lines was found to be more precise for DRI zones investigated up to an average depth of 420 mm. On the other hand, the simple random sampling plan was more precise for DRI zones deeper in the component. Then, the thereby calculated standard deviation was multiplied by the correction factor related to the average depth of the investigated zone (Table 4.1). A statistical/probabilistic approach to compare confidence intervals provided in this study is shown in Figure 4.2.

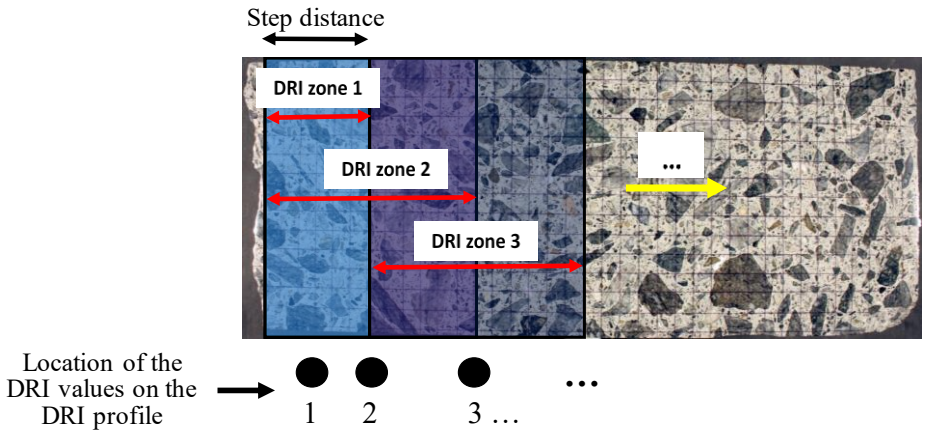

Figure 4.1: Procedure used to assess the internal damage profile within a core extracted from a structure [18].

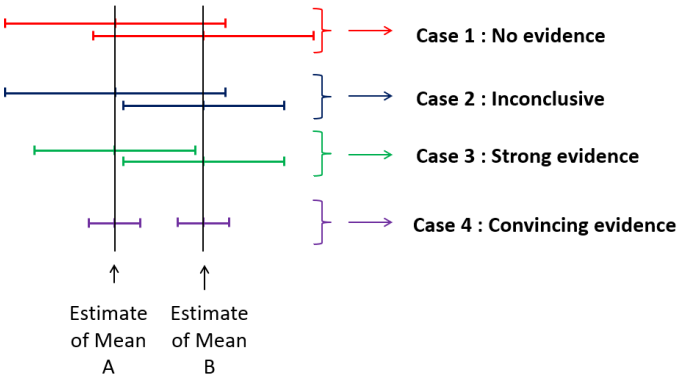

Figure 4.2: Statistical/probabilistic methodology used to compare the DRI numbers with their respective confidence interval, adapted from Ramsey and Schafer [24].

5. RESULTS

The DRI damage profile of the entire core is shown in Figure 5.1A with a colour code corresponding to the damage classification for ASR suggested by Sanchez et al. [13]. Figure 5.1B also shows a scaled picture of the whole polished section. The reference surface on the left corresponds to the downstream face and is exposed to atmospheric conditions, i.e. freeze/thaw and wetting/drying. The opposite side of the core along the inner 250 mm (to the right in Figure 5.1B) is most likely part of the slab dam (see Figure 3.1A), as a "cold joint" has been observed between the two parts of the dam.

There are convincing (statistically) evidences that the internal damage varies significantly from the downstream to the upstream face, which is highlighted in Sections I to VI in Figure 5.1A and illustrated in Figure 5.1C and 5.1D. Section I starts at the downstream face with a marginal/moderate damage degree, which increased drastically until reaching a plateau at a depth of about 100 to 200 mm where a very high damage degree was found. Then, a drastic decrease in damage is observed until reaching the 300-mm depth where Section II begins. A relatively constant damage degree was found until reaching about 850 mm in depth. Then a second steep drop of damage is observed towards the beginning of Section III where it remained relatively constant from about 1000 mm until reaching about 1550 mm in depth. A third significant damage drop was then found between 1550 and 1700 mm (beginning of Section IV) to re-increase and reach the same damage degree as in Section III (DRI of about 400) and remain at that level from 1875 to 2150 mm (Section V). In Section VI, at a depth of 100 mm from the end of the core, the damage degree increased significantly up to a moderate damage degree.

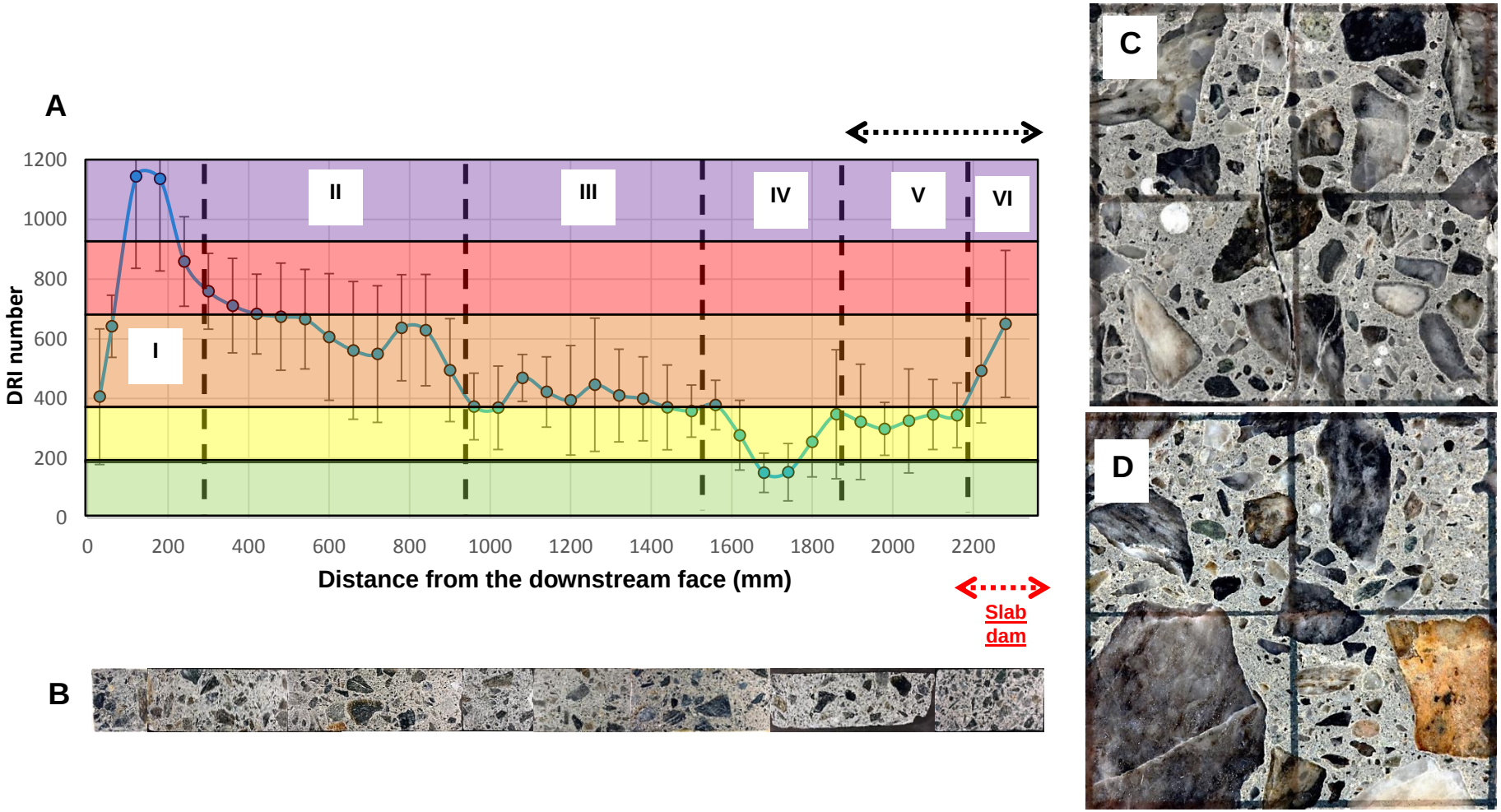

Figure 5.1: (A) Internal damage profile obtained with the DRI method on the core extracted from the lower part of Votna I abutment wall. The profile was divided in Sections I to VI to highlight the main variations in damage degree. The reference surface (left) is the downstream face (see Figure 2.1). The black arrow indicates the presence of water close to the coring location (≈ 100 mm) upstream. The colour code refers to an approximate damage classification for ASR based on the one provided by Sanchez et al. [13] (Table 1.2) : negligible (green), marginal (yellow), moderate (orange), high (red), very high (purple). (B) Scaled picture of the six polished specimens showing the aggregate particles distribution. (C) Typical micrographs showcasing damage due to ASR at a distance of 150 mm (DRI ≈ 1200) and (D) 1700 mm (DRI ≈ 180) from the downstream face.

6. DISCUSSION

6.1 Explaining the damage variations

Because the core was extracted parallel to the connection point between the slab dam and the abutment wall (see Figure 2.1), the loading and stress concentrations were presumably quite similar through the cross-section. Therefore, it was expected to observe damage variations at the meter scale only, especially when approaching the upstream face where an increased moisture availability would likely increase the damage degree. However, the damage profile shows variations at the scale of one hundred mm within the assessed component, with six significant damage variations over the whole 2.3 meters length of the core (Sections I to VI). This confirms that assessing the degree of damage within a fairly thick structural component based on DRI determinations (or any other damage assessment tool such as the Stiffness Damage Test for instance) obtained from a 200/300 mm-long core taken from the surface or actually at any depth in the component may provide a misleading picture of the overall condition of that structural element. Furthermore, Figure 5.1B shows that the aggregate particles distribution is very heterogeneous, which does not seem to explain localized damage discontinuities per se. Based on the damage assessment only, it is very difficult to draw comprehensive conclusions on why internal damage varied in such a way within the element examined. However, some assumptions can be provided based on previous work.

When looking at the core sections close to the downstream surface (Section I), one can see how exposure conditions affects concrete damage. In Section I, the low damage in the first about 50 mm (DRI of 500) is probably related to the alkali leaching previously documented in the surface layer of a concrete element exposed to atmospheric conditions [19]. The rapidly increasing damage over the first 200 mm (DRI of 1150) is likely related to the influence of freeze-thaw, in conjunction with ASR, which induced a significantly higher damage degree for the first 200 mm. This is in accordance with the observations of Sanchez et al. [25] who determined higher DRI numbers on laboratory specimens damaged by ASR and freeze/thaw than on corresponding specimens of equal expansion damaged only by ASR. Although in Section I the cracks were larger, abundant and parallel to the surface (as normally observed in cores with sign of internal freeze/thaw damage), the observed petrographic features indicated damage resulting from ASR (i.e. cracks located in the reactive aggregate particles) rather than freeze/thaw only (Figure 5.1C). This suggests that ASR and freeze/thaw potentially interacted altogether to generate such damage degree close to the downstream surface (i.e. < 200 mm) and form an “hybrid” damage pattern. This kind of damage pattern was also noticed before in the upper part of the Sartigan dam (Canada) by Fournier [26]. These observations are also supported by the increased moisture state, measured by degree of capillary saturation (DCS) and internal relative humidity (RH) using the procedures introduced by Lindgård et al. [27], closer to the downstream face compared to deeper in the structure (Figure 6.1). Furthermore, and through that whole 400-mm portion of the core, the PF (*Pore protection*) factor measured with the Finnish Standard SFS 4475 (“PF method”) [28] is much lower than the recommended 0.20 value, which indicates a vulnerability to freeze/thaw damage [29]. The lack of influence of freeze/thaw between 200 and 300 mm thereby explains the gradual decrease of damage over the last portion of Section I.

In the last portion of the core (Section VI), the damage degree increased significantly within the last 100 mm, which interestingly corresponds to the magnitude of the damage drop observed between Sections II and III. It is not expected to be related to a change of exposure conditions, since the last 500 mm of the core (Sections V and VI) had similar exposure conditions; this last 500 mm-long portion of the core was located very close to the submerged area where water is highly available all year long (see section 3.2). Alkali leaching has not likely influenced the damage degree in that portion of the core since Plusquellec et al. [19] documented that leaching only affected the concrete in the first 100 mm from the water exposed upstream face of the Votna I dam [19]. However, alkali leaching might have affected (reduced) the damage in the outermost portion (Section I) of the core towards the downstream face. The reason for this local increase in damage in the deepest portion of the core might be connected to a change of concrete mix design between the slab dam and the abutment wall. Visual observations of the dam during repair and of the block at Voll indicates that the slab dam was cast after the abutment wall and the arch dam, and that there is a “joint” between them. This is also supported by the presence of two rebars very close to one another in Section VI (Figure 3.2).

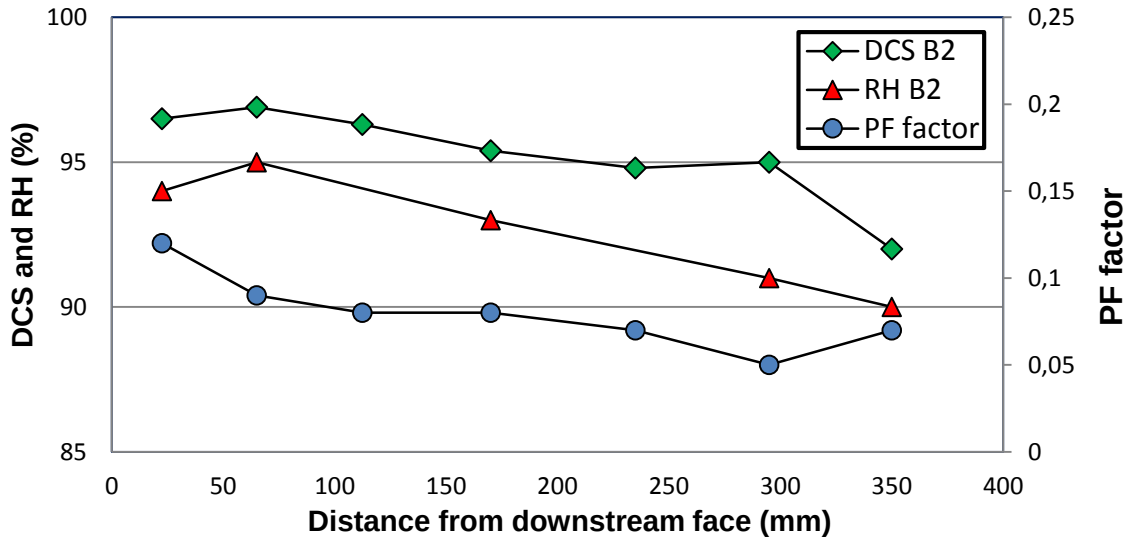

Figure 6.1: Degree of capillary saturation (DCS), internal relative humidity (RH) and PF factor profiles obtained from a companion core extracted from the abutment wall. The reference surface (left) is the downstream face (see Figure 2.1), adapted from Lindgård et al. [30].

What happens internally in Sections II to V likely needs to be assessed from a much larger point-of-view and probably cannot be essentially explained by variations in the exposure conditions but may rather involve the effect of restraints/loadings. The effect of restraint on ASR-induced expansion was studied by many authors (e.g. [31–37]) who showed that expansion is significantly reduced in the direction of stress. Moreover, Dunant and Scrivener's [37] model suggests that loading affects the kinetics of ASR and cracking in the aggregate particles occurs earlier when stress is applied. This suggests that, for equal expansion, the resulting damage degree is enhanced when a load is applied. In the case of dams, it is fairly well acknowledged that the combined effect of anisotropic restraints, temperature variations (and the associated thermal stress) and different exposure to moisture cause anisotropic expansion (and the associated stress) and relative displacements within different portions of the structure [38]. The resulting stresses applied to the structure are heterogenous and difficult to assess, which requires advanced numerical modelling to assist in the structural evaluation of the affected dams [38]. For instance, Léger et al. [39] and Sellier et al. [40] showed the heterogenous tensile/compressive stresses within ASR-affected dams at a large scale and the resulting surface cracking using finite element modelling. However, the resulting effects on internal cracking still remains largely unexplored. The internal damage profile in Figure 5.1A shows that significant damage variations can be expected at the scale of approximately one hundred mm possibly due to anisotropic restraints and the resulting heterogeneous tensile/compressive stresses applied locally. Furthermore, one cannot rule out that local variations in the concrete alkali content due to varying cement content might contribute to local variations in damage. The localized low damage degree in Section IV (Figure 5.1D) actually corresponds to the presence of the only observed reinforcing bar parallel to the axis of the core (see the fourth section of the core in Figure 3.2), thus providing an additional indication supporting the above theory.

6.2 Sensitivity of the DRI method for the spatial damage assessment of field specimens

Provided the same operator performs the analysis, this study shows that the spatial damage assessment tool developed by Champagne [18] offers a reliable approach to qualitatively assess damage variations within structure components, even at the scale of one hundred mm. However, the precision level of the obtained DRI numbers can be rather low if a single core is used for the determination of the internal damage profile, as shown in Figure 5.1A. This indicates that damage variations must be substantial in the investigated component location to be able to detect them with the DRI method at such a small scale. However, a way to significantly improve the precision of that approach (by approximately twice) is to perform the analysis on the same number of squares but from two cores extracted parallel to one another at the investigated location. Thus, by avoiding the use of the correction factor applied to the standard deviation (Table 4.1), the precision is relatively improved by that factor, which is considerable.

7. SUMMARY AND CONCLUSION

This paper presented a case study where the Damage Rating Index (DRI) method was applied for spatial analysis and the establishment of an internal damage profile from the examination of a core extracted from an ASR-affected concrete structure component. The above long DRI profile is obtained by segmenting the extracted core in *DRI zones* of similar area within the polished section examined, and by assessing their respective DRI number. Using the above damage spatial analysis approach, the internal damage profile along a 2.3m-long core extracted from the lower part of the abutment wall of an ASR-affected dam in the south-western part of Norway was determined. The extracted core passed through the whole component, from the downstream (exposed to atmospheric conditions) face towards the upstream face very close to the submerged area of the dam.

The results of the DRI determination showed that internal damage varied significantly at the scale of one hundred mm within the assessed component, which is assumed to be caused by the combined influence of ASR and freeze/thaw action at the downstream surface and possibly to anisotropic restraints inside the dam (and the resulting heterogeneous tensile/compressive stresses). The main conclusion of this study is that assessing the internal damage within a concrete component can provide much valuable information, which will likely be more representative of the (variations in the) internal condition of that component than that obtained from the testing of a “short” specimen extracted from the surface of that element.

8. ACKNOWLEDGEMENTS

The authors would like to acknowledge Hydro Energy AS that has funded the transportation of the block from the dam site to Trondheim and the coring of the long core examined. We will also acknowledge the financial support from the Norwegian research project 236661 "Alkali-silica reaction in concrete – reliable concept for performance testing" (mainly funded by the Norwegian Research Council) that has funded the transportation costs to Canada and partly the PhD research of the main author, in addition to SINTEF's and NTNU's work on the project.

9. REFERENCES

1. Wood JGM, Johnson RA (1993) The Appraisal and Maintenance of Structures with Alkali-Silica Reaction. The Structural Engineer 71:19–23

2. Shrimer FH (2000) Application and use of Damage Rating Index in assessment of AAR-affected concrete - Selected case studies. In: Proceedings of the 11th International Conference on Alkali-Aggregate Reaction (ICAAR). Québec City (Canada). Québec City (Canada), pp 899–907

3. Sanchez LFM, Fournier B, Jolin M, Duchesne J (2015) Reliable quantification of AAR damage through assessment of the Damage Rating Index (DRI). Cement and Concrete Research 67:74–92. http://dx.doi.org/10.1016/j.cemconres.2014.08.002

4. Champagne M (2020) Applying the Damage Rating Index for the spatial damage assessment in concrete specimens affected by alkali-silica reaction (ASR). MSc Thesis, Université Laval

5. Grattan-Bellew PE, Danay A (1992) Comparison of laboratory and field evaluation of alkali-silica reaction in large dams. In: International Conference on Concrete Alkali-Aggregate Reactions in Hydraulic Plants and Dams. Fredericton (Canada), pp 1–23

6. Villeneuve V, Fournier B, Duchesne J (2012) Determination of the damage in concrete affected by ASR - The Damage Rating Index (DRI). In: Proceedings of the 14th International Conference on Alkali-Aggregate Reaction (ICAAR). Austin (Texas). Austin (Texas), p 10

7. Monette LJ, Gardner NJ, Grattan-Bellew PE (2002) Residual Strength of Reinforced Concrete Beams Damaged by Alkali-Silica Reaction—Examination of Damage Rating Index Method. ACI Materials Journal 99:. https://doi.org/10.14359/11315

8. Rivard P, Ballivy G (2003) Application de méthodes pétrographiques à l'évaluation de l'état de dégradation du béton affecté par l'alcali-réaction. Bulletin des laboratoires des Ponts et Chaussées 244–245:73–90

9. Hagelia P (2004) Origin of map cracking in view of the distribution of air voids, strength and ASR-gel. In: Proceedings of the 12th International Conference on Alkali-Aggregate Reaction (ICAAR). Beijing, China, p 12

10. Grattan-Bellew PE (2012) Petrographic methods for distinguishing between alkali-silica, alkali-carbonate reactions and other mechanisms of concrete deterioration. In: Proceedings of the 14th International Conference on Alkali-Aggregate Reaction (ICAAR). Austin (Texas), p 10

11. Grattan-Bellew PE, Mitchell LD (2006) Quantitative Petrographic Analysis of Concrete – The Damage Rating Index (DRI) Method, A Review. In: 8th CANMET/ACI Int. Conf. on Recent Advances in Concrete Technology. Montreal (Canada), p 14

12. Powers LJ, Shrimer FH (2007) Quantification of ASR in concrete: An introduction to the Damage-Rating Index method. In: Proceedings of the 29th Cement Microscopy International Conference (ICMA). Montreal (Canada). International Cement Microscopy Association, Montreal (Canada), pp 345–353

13. Sanchez LFM, Fournier B, Jolin M, et al (2017) Overall assessment of Alkali-Aggregate Reaction (AAR) in concretes presenting different strengths and incorporating a wide range of reactive aggregate types and natures. Cement and Concrete Research 93:17–31. https://doi.org/10.1016/j.cemconres.2016.12.001

14. Sanchez LFM, Fournier B, Jolin M, et al (2017) Overall assessment of Alkali-Aggregate Reaction (AAR) in concretes presenting different strengths and incorporating a wide range of reactive aggregate types and natures. Cement and Concrete Research 93:17–31. https://doi.org/10.1016/j.cemconres.2016.12.001

15. Gautam BP, Panesar DK (2017) The effect of elevated conditioning temperature on the ASR expansion, cracking and properties of reactive Spratt aggregate concrete. Construction and Building Materials 140:310–320. https://doi.org/10.1016/j.conbuildmat.2017.02.104

16. Deschenes R, Giannini ER, Drimalas T, et al (2018) Mitigating Alkali-Silica Reaction and Freezing and Thawing in Concrete Pavement by Silane Treatment. ACI Materials Journal 115:. https://doi.org/10.14359/51702345

17. Fournier B, Fecteau P-L, Villeneuve V, et al (2015) Description of petrographic features of damage in concrete used in the determination of the Damage Rating Index (DRI). Département de géologie et de génie géologique, Université Laval

18. Champagne M Use of statistical approaches for the analysis of Damage Rating Index (DRI) data for the condition assessment of ASR-affected concrete structures. PhD Thesis in preparation, Université Laval

19. Plusquellec G, Geiker MR, Lindgård J, De Weerdt K (2018) Determining the free alkali metal content in concrete – Case study of an ASR-affected dam. Cement and Concrete Research 105:111–125. https://doi.org/10.1016/j.cemconres.2018.01.003

20. Rodum E, Lindgård J, Thorenfeldt E (2005) Dam I Votna – Testing of cored concrete. Restricted report by SINTEF Building and Infrastructure, Trondheim (Norway)

21. Larsen S, Lindgård J, Thorenfeldt E, et al (2008) Experiences from extensive condition survey and FEM-analyses of two Norwegian concrete dams with ASR. In: Proceedings of the 13th International Conference on Alkali-Aggregate Reaction (ICAAR). Trondheim (Norway), p 10

22. Sanchez L, Fournier B, Jolin M, et al (2016) Use of Damage Rating Index to Quantify Alkali-Silica Reaction Damage in Concrete: Fine versus Coarse Aggregate. ACI Materials Journal 113:395–407. https://doi.org/10.14359/51688983

23. Lohr SL (2010) Cluster Sampling with Equal Probabilities. In: Sampling: Design and Analysis, Second edition. Brooks/Cole, Boston, MA 02210, pp 165–218

24. Ramsey F, Schafer D (2002) Comparisons Among Several Samples. In: The Statistical Sleuth A Course in Methods of Data Analysis, 2nd Edition. Cengage Learning, Boston, MA 03310

25. Sanchez LFM, Drimalas T, Fournier B (2020) Assessing condition of concrete affected by internal swelling reactions (ISR) through the Damage Rating Index (DRI). Cement 1–2:100001. https://doi.org/10.1016/j.cement.2020.100001

26. Fournier B (2014) Programme d'investigation relatif à l'alcali-réaction au barrage Sartigan. Département de géologie et de génie géologique de l'Université Laval, Rapport final remis au Centre d'Expertise hydrique du Québec, Département de géologie et de génie géologique, Université Laval, July 2014, 150p.

27. Lindgård J, Rodum E, Pedersen B (2006) Alkali-Silica Reactions in Concrete – Relationship between Water Content and Observed Damage on Structures. In: 7th CANMET/ACI International conference on Durability of Concrete. Montreal, Canada, p 147-165

28. Finnish Standard SFS 4475 (1980) Suomen Standardisoimisliitto. Helsinki

29. Sellevold EJ, Farstad T (2005) The PF-method – A Simple Way to Estimate the w/c-ratio and Air content of Hardened Concrete. ConMat'05 and Mindness Symposium, University of British Colombia, Vancouver, Canada, ISBN: 0-88865-810-9.

30. Lindgård J, Hammer TA, Skjølsvold O, et al (2017) 236661 KPN-ASR - Test report 1. SINTEF Building and Infrastructure, Trondheim (Norway)

31. Larive C, Laplaud A, Joly M (1996) Behaviour of AAR affected concrete: Experimental data. In: Proceedings of the 11th International Conference on Alkali-Aggregate Reaction (ICAAR). Melbourne, Australia, pp 670–677

32. Multon S, Toutlemonde F (2006) Effect of applied stresses on alkali–silica reaction-induced expansions. Cement and Concrete Research 36:912–920. https://doi.org/10.1016/j.cemconres.2005.11.012

33. Grimal E, Sellier A, Pape YL, Bourdarot E (2008) Creep, Shrinkage, and Anisotropic Damage in Alkali-Aggregate Reaction Swelling Mechanism-Part II: Identification of Model Parameters and Application. MJ 105:236–242. https://doi.org/10.14359/19819

34. Grimal E, Sellier A, Pape YL, Bourdarot E (2008) Creep, Shrinkage, and Anisotropic Damage in Alkali-Aggregate Reaction Swelling Mechanism-Part I: A Constitutive Model. MJ 105:227–235. https://doi.org/10.14359/19818

35. Herrador MF, Martínez-Abella F, Rabuñal Dopico JR (2008) Experimental evaluation of expansive behavior of an old-aged ASR-affected dam concrete: methodology and application. Mater Struct 41:173–188. https://doi.org/10.1617/s11527-007-9228-y

36. Berra M, Faggiani G, Mangialardi T, Paolini AE (2010) Influence of stress restraint on the expansive behaviour of concrete affected by alkali-silica reaction. Cement and Concrete Research 40:1403–1409. https://doi.org/10.1016/j.cemconres.2010.05.002

37. Dunant CF, Scrivener KL (2012) Effects of uniaxial stress on alkali–silica reaction induced expansion of concrete. Cement and Concrete Research 42:567–576. https://doi.org/10.1016/j.cemconres.2011.12.004

38. Léger P, Tinawi R, Mounzer N (1995) Numerical simulation of concrete expansion in concrete dams affected by alkali–aggregate reaction: state-of-the-art. Can J Civ Eng 22:692–713. https://doi.org/10.1139/l95-081

39. Léger P, Côté P, Tinawi R (1996) Finite element analysis of concrete swelling due to alkali-aggregate reactions in dams. Computers & Structures 60:601–611. https://doi.org/10.1016/0045-7949(95)00440-8

40. Sellier A, Bourdarot E, Multon S, et al (2009) Combination of Structural Monitoring and Laboratory Tests for Assessment of Alkali-Aggregate Reaction Swelling: Application to Gate Structure Dam. MJ 106:281–290. https://doi.org/10.14359/56553